

## INTERPRETATION OF SPATIAL AUTOCORRELATION METHOD BASED ON THE THEORY OF SEISMIC INTERFEROMETRY

T. Yokoi<sup>1</sup> and S. Margaryan<sup>2</sup>

<sup>1</sup> Senior Research Scientist, International Institute of Seismology and Earthquake Engineering,  
Building Research Institute, Tsukuba, Japan  
Email: tyokoi@kenken.go.jp

<sup>2</sup> Senior Researcher, Laboratory of Applied Geology, Yerevan State University, Yerevan, Armenia  
Email: msos78@hotmail.com

### ABSTRACT :

In this paper, first we show the theoretical cross-check of SPatial AutoCorrelation method (SPAC) and Seismic Interferometry: the retrieval of the elastodynamic Green's function. Their mutual consistency is almost complete. The only discrepancy is found on the average of the complex coherence function over azimuth in wave field dependent on azimuth. It is guessed in discussion that the discrepancy is owed by the way of representing wave field in the back ground theory of Seismic Interferometry that can produce only wave field moderately dependent on azimuth, and that the mentioned consequences of Seismic Interferometry also can make sense only in wave field moderately dependent on azimuth.

Then, we show the result of the numerical experiments using the simulated microtremor records for given horizontally layered structures in order to confirm the formulas foreseen by the Seismic Interferometry to calculate the phase velocity in case of mixture of the fundamental and the first higher modes of Rayleigh waves, in that the eigen functions of both modes play the role of combining the their effects. The result clearly showed that these formulas can reproduce well the dispersion curves obtained by the conventional way of analysis by SPAC and Centerless Circular Array Method and therefore supports the way to estimate quantitatively the effect of the first higher mode on the dispersion curve.

**KEYWORDS:** Microtremor, Seismic Interferometry, SPatial AutoCorrelation Method, Centerless Circular Array Method, Multiple Modes, Dispersion Curve

## 1. INTRODUCTION

After the original theory of SPAC method given by the pioneering work of Aki (1957), the methods based on correlation analysis of microtremor field has been developed for about fifty years and among them SPAC established by Okada (2003). A huge number of successful examples of application can be found in the journals and the proceedings of the conferences of the related study fields. One of the notable recent topics is the effect of the array pattern or the possibility of run-off (*e. g.*, Bettig *et al.* 2001; Ohori *et al.* 2002; Morikawa *et al.* 2004; Ohrnberger *et al.* 2004; Chávez-García *et al.* 2005; Chávez-García *et al.* 2006; Köhler *et al.* 2007) from the standard equilateral triangular array that was proposed by Okada (2003) and of which optimum was newly confirmed by Okada (2006) and Asten (2006). On the other hand, Cho *et al.* (2006a; 2006b) and Tada *et al.* (2007) have proposed a series of new techniques based on the generic formulation for circular microtremor array. Among them Centerless Circular Array method (CCA) is focused on as well as SPAC in this paper in relation with another recently developed big research topic Seismic Interferometry, especially the retrieval of the elastodynamic Green's function from correlation of the microtremor wave field.

A pioneering work had appeared in earlier times (*e. g.*, Claerbout 1968). This has been consciously recognized mainly in the new century. Detailed reviews are given, *e. g.*, by Sabra *et al.* (2005a; 2005b), Sanchez-Sesma and Campillo (2006), Wapenaar *et al.* (2006). The successful experimental results (*e. g.*, Sabra *et al.* 2005a, 2006b; Shapiro and Campillo 2004), and the theoretical ones (*e. g.*, Snieder 2004) are categorized in the case of surface waves in the short wave length range, its typical wave length is shorter than its site interval. In this paper, we focus on SPAC of which wave length is comparable or longer than the interval between sites. The stationary phase approximation used by Snieder (2004) is not applicable for our case.

Wapenaar and Fokkema (2006) show the following with point sources located along the buried surface.

$$2 \operatorname{Re} \left\{ \hat{G}_{p,q}^{v,t} (x_A, x_B, \mathbf{w}) \right\} \mathcal{S}(\mathbf{w}) \approx 2 \left\langle \left\{ \hat{v}_p^{obs} (x_A, \mathbf{w}) \right\}^* \cdot \hat{v}_q^{obs} (x_B, \mathbf{w}) \right\rangle / \mathbf{r}_d c_p, \quad (1.1)$$

where the right member is the cross spectra of the observed particle velocity at  $x_A$  and  $x_B$  on the free surface,  $\langle \rangle$  denotes a spatial *ensemble* average, asterisk at superscript the complex conjugate,  $S(\mathbf{w})$  the power spectra that is assumed to be the same for all sources, the contents of  $\{ \}$  in the left member the elastodynamic Green's functions in the frequency domain that is the  $p$ -th component of particle velocity observed at  $x_A$  due to an unit traction force applied to the  $q$ -th direction at  $x_B$ ,  $\operatorname{Re}\{ \}$  the real part of the complex quantity,  $\mathbf{r}_d$  and  $c_p$  the density and P-wave velocity respectively on and outside of the buried surface that are isotropic and homogeneous. The left member is equal to the sum of the causal and the acausal ones.

Yokoi and Margaryan (2008) have shown the consistency of the SPAC theory and Seismic Interferometry that is almost complete except on the necessity of the average over azimuth as shown below.

## 2. CONSISTENCY OF SPAC METHOD WITH THE SEISMIC INTERFEROMETRY

Replace the *ensemble* average of the cross spectra in the right member of Eqn.(1.1) with that over the time, relying on the stochastic features of observed microtremor (Okada 2003). The corresponding complex coherence function is given as follows.

$$(\mathbf{g}_z)_{A,B} = \frac{\left\langle \left\{ \hat{v}_z^{obs} (x_A, \mathbf{w}) \right\}^* \hat{v}_z^{obs} (x_B, \mathbf{w}) \right\rangle}{\left\langle \left\{ \hat{v}_z^{obs} (x_A, \mathbf{w}) \right\}^* \hat{v}_z^{obs} (x_A, \mathbf{w}) \right\rangle} \approx \frac{-2 \operatorname{Re} \left\{ \hat{G}_{z,z}^{v,t} (x_A, x_B, \mathbf{w}) \right\} \mathcal{S}_v(\mathbf{w})}{-2 \operatorname{Re} \left\{ \hat{G}_{z,z}^{v,t} (x_A, x_A, \mathbf{w}) \right\} \mathcal{S}_v(\mathbf{w})} = \frac{\operatorname{Re} \left\{ \hat{G}_{z,z}^{v,t} (x_A, x_B, \mathbf{w}) \right\}}{\operatorname{Re} \left\{ \hat{G}_{z,z}^{v,t} (x_A, x_A, \mathbf{w}) \right\}}. \quad (2.1)$$

The noise power spectra are canceled out as well as other proportionality factors. Therefore, the complex coherence function  $(\mathbf{g}_z)_{A,B}$  is represented only by the elastodynamic Green's functions and depends only on the underground velocity structure. In case of horizontally layered media, this complex coherence function becomes independent on azimuth.

Assume the dominance of the contribution of the poles in the complex wavenumber plane that corresponds to the normal modes at long distance. In general, the vertical component of the Green's function for horizontally layered media does contain the reflected and refracted body waves. It, however, seems appropriate because both of the force and the receiver are located at the free surface. This assumption gives

$$\hat{G}_{z,z}^{v,t}(x_A, x_B, \mathbf{w}) \approx -\mathbf{w} \sum_{n=0}^{\infty} \{\hat{r}_2(k_n, 0)\}^2 J_0(k_n r_{A,B}), \quad (2.2)$$

where the subscript  $n$  shows the mode numbering, the content of  $\{ \}$  is the eigen function for vertical component normalized by the phase and group velocities and the energy integral (Yokoi and Margaryan 2008). This can be derived from the formulas of surface waves Green's tensors without being applied the far field approximation (*e. g.*, Aki and Richard 2002).

Assuming that the fundamental mode is dominant over the summation gives the following.

$$(\mathbf{g}_z)_{A,B} \approx \text{Re} \left\{ \left[ \hat{r}_2(k_0, 0) \right]^2 J_0(k_0 r_{A,B}) \right\} / \text{Re} \left\{ \left[ \hat{r}_2(k_0, 0) \right]^2 J_0(0) \right\} = J_0(k_0 r_{A,B}), \quad (2.3)$$

where the wavenumber  $k_0$  corresponds to the fundamental mode of Rayleigh wave, because  $J_0(z)$  is unity at  $z=0$ . Note that the information of the site dependent amplification is canceled out. Averaging both members of Eqn.(2.3) over azimuth the conventional formula of SPAC coefficient is reproduced.

If the fundamental and the first higher modes are considerable, the following is derived from Eqn.(2.2).

$$(\mathbf{g}_z)_{A,B} = \mathbf{b} \cdot J_0(k_0 r_{A,B}) + (1 - \mathbf{b}) \cdot J_0(k_1 r_{A,B}), \quad \mathbf{b} = \text{Re} \left\{ \left[ \hat{r}_2(k_0, 0) \right]^2 \right\} / \left\{ \text{Re} \left[ \hat{r}_2(k_0, 0) \right]^2 + \text{Re} \left[ \hat{r}_2(k_1, 0) \right]^2 \right\}. \quad (2.4)$$

Note that Eqn.(2.4) is different from Tokimatsu *et al.*(1992) as Eqn.(2.2) shows clearly.

Starting from Eqn.(1.1), the same formulas as those derived by SPAC theory for vertical component are obtained. For horizontal components, the conventional formulas (Okada 2003) similarly can be given as shown by Yokoi and Margaryan (2008). Seismic Interferometry gives the consequence that is almost completely consistent with SPAC method and its background theory. The only one discrepancy is found on the average over azimuth. The theoretical foresight Eqn.(2.3) suggests that the complex coherence function can be used in place of SPAC coefficient. Yokoi and Margaryan (2008) have shown an example of field data for that this foresight is accompanied with the deviation of dispersion curves that, however, is acceptable (Figure 2.1).

They finally conclude that the discrepancy is owed by the way of representation of Wapenaar and Fokkema (2006) that can not express wave field so strongly dependent as a plane wave coming from one direction and that in moderately azimuth dependent wave field Seismic Interferometry can make sense. A consideration similar as Eqn.(2.4) can be done for CCA method as shown below.

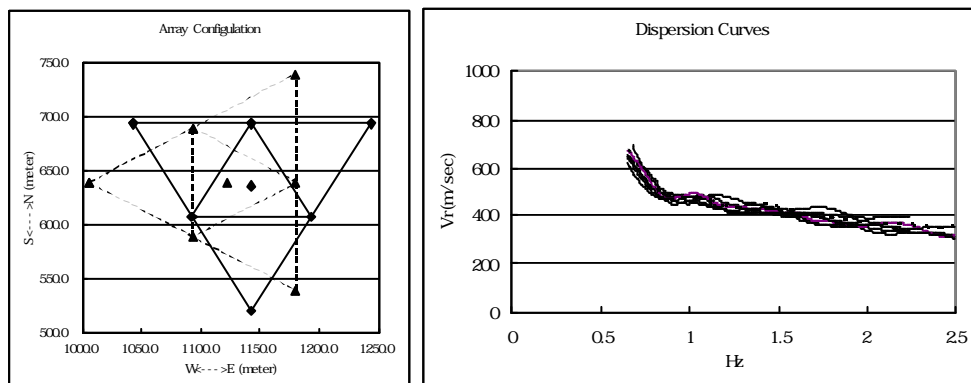


Figure 2.1 *Left*: Configuration of doubled arrays. *Right*: Dispersion curves obtained from the real part of the complex coherence functions corresponding to six directions and those from SPAC coefficients (Yokoi and Margaryan 2008).

### 3. APPLICATION OF SEISMIC INTERFEROMETRY TO CENTERLESS CIRCULAR ARRAY

The coefficient for CCA corresponding to SPAC's one is as follows (Cho *et al.* 2006 a, 2006b; Tada *et al.* 2007).

$$s(r, \mathbf{w}) = \frac{G_{z_0z_0}(r, r; \mathbf{w})}{G_{z_1z_1}(r, r; \mathbf{w})} = \frac{PSD \left\langle \int_{-p}^p Z(t, r, \mathbf{q}) d\mathbf{q} \right\rangle}{PSD \left\langle \int_{-p}^p Z(t, r, \mathbf{q}) \exp(-i\mathbf{q}) d\mathbf{q} \right\rangle} = \frac{J_0^2(r\mathbf{w}/c)}{J_1^2(r\mathbf{w}/c)}, \quad (3.1)$$

where  $G_{z_0z_0}$  and  $G_{z_1z_1}$  denotes the power spectral density of the zero and the first order's coefficients of Fourier expansion over azimuth of  $Z(t, r, \mathbf{q})$  that is the vertical component of microtremor observed at the radius  $r$  and at the time  $t$ ,  $J_1(\cdot)$  the first kind Bessel function of the first order,  $PSD \langle \rangle$  power spectral density.

Cho *et al.* (2006a) have shown the following formula for cases of multiple modes.

$$G_{z_0z_0}(r, r; \mathbf{w})/G_{z_1z_1}(r, r; \mathbf{w}) = \sum_{i=0}^M \mathbf{a}_i(\mathbf{w}) J_0^2(k_i r) / \sum_{i=0}^M \mathbf{a}_i(\mathbf{w}) J_1^2(k_i r), \quad \mathbf{a}_i(\mathbf{w}) = f_i(\mathbf{w})/f(\mathbf{w}), \quad f(\mathbf{w}) = \sum_{i=1}^M f_i(\mathbf{w}), \quad (3.2)$$

where  $\mathbf{a}_i(\mathbf{w})$  is the power partition ratio for the  $i$ -th mode,  $f(\mathbf{w})$  the power in total,  $f_i(\mathbf{w})$  the power of the  $i$ -th mode. (1.1) can be applied for autocorrelation also. Therefore, the power of vertical component is given by the elastodynamic Green's function. Then, assume the dominance of the contribution of the poles as above. The power partition for each mode can be described as follows.

$$\left\langle \left\{ \hat{v}_z^{obs}(x_A, \mathbf{w}) \right\}^* \cdot \hat{v}_z^{obs}(x_A, \mathbf{w}) \right\rangle \approx -\hat{r}_c \mathbf{w} \hat{S}(\mathbf{w}) \sum_{n=0}^{\infty} \left\{ \hat{r}_2(k_i, 0) \right\}^2. \quad (3.3)$$

Namely, the square of the normalized eigen function represents the power partition ratio. Then,

$$\mathbf{a}_i(\mathbf{w}) = \left\{ \hat{r}_2(k_i, 0) \right\}^2 / \sum_{n=0}^{\infty} \left\{ \hat{r}_2(k_i, 0) \right\}^2. \quad (3.4)$$

Assuming  $M=1$  that means the fundamental and the first modes is dominant the following is obtained.

$$s(r, \mathbf{w}) = \frac{G_{z_0z_0}(r, r; \mathbf{w})}{G_{z_1z_1}(r, r; \mathbf{w})} = \frac{\mathbf{b}_0 J_0^2(k_0 r) + \mathbf{b}_1 J_0^2(k_1 r)}{\mathbf{b}_0 J_1^2(k_0 r) + \mathbf{b}_1 J_1^2(k_1 r)}, \quad \mathbf{b}_0 = \text{Re} \left\{ \hat{r}_2(k_0, 0) \right\}^2, \quad \mathbf{b}_1 = \text{Re} \left\{ \hat{r}_2(k_1, 0) \right\}^2 \quad (3.5)$$

### 4. NUMERICAL EXAMPLES

Two sets of synthetic microtremor records provided for *NBT*, *i. e.*, N101 and N104 are used. *NBT* is referred by *Noise Blind Test* in *Third International Symposium on the Effect of Surface Geology on Seismic Motion* (ESG2006) (Cornou *et al.* 2006). These are calculated and provided to the participants of *NBT* using the finite difference codes developed by Moczo and Kristec (2002) for the given horizontally layered media. These are not isotropic or dominated by the fundamental mode, moreover free from the problem due to different system characteristics among channels, then the performance of the method CCA itself can be checked.

#### 4.1 Performance of CCA in comparison with SPAC

Using the data set N101, the performance of CCA with six stations of the radius 6m is shown at first in comparison with SPAC with fifteen stations of the maximum radius 89m.

The provided array configuration is shown in the right panel of Figure 4.1 *left*. The radii are 6m, 23m and 89m for the inner and middle hexagons and the outer triangle, respectively. The records obtained at these fifteen stations were used all together for SPAC analysis. The duration of the provided records is about eleven minutes and whole dataset were used. The dispersion curve determined using SPAC is shown by gray dots in Figure 4.1 *right*, whereas the black dots shows that determined using CCA with the six stations composing the inner hexagon. This very good coincidence shows CCA with six stations of radius 6m can play the almost same role of SPAC with fifteen stations of the maximum radius 89m. Namely, we can consider them the different ways to obtain the same dispersion curve.

They, however, showed together a systematic run off from the theoretical dispersion curve of the fundamental mode for the given structure as shown in Figure 4.1 *right*. They lay together between the fundamental and the first higher modes (black and gray curves respectively). This problem is solved using Eqn. (3.5) as shown below.

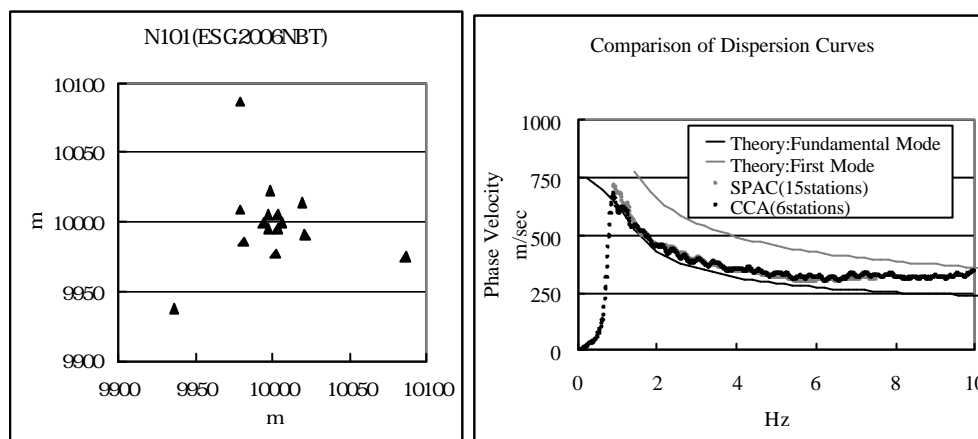


Figure 4.1 N101 case. *Left*: configuration of array. *Right*: Comparison of the dispersion curves. one determined by 6 station CCA (black dots), another 15 station SPAC (gray dots). Black and gray smooth curves denote the fundamental and the first higher modes of Rayleigh waves, respectively.

#### 4.2 Validation of the theoretical foresight

Here, the validation of Eqn.(3.5) is shown using the simulated records. The procedure of data processing applied is as follows. It seems conservative in comparison with practitioner's one.

The SPAC coefficients are converted to the phase velocity using the fifth order polynomial that approximates the inverse function of the first kind Bessel function of the zero order  $J_0(kr)$  in the range of  $kr$  where  $J_0(kr)$  does not start oscillating and takes only one value. Once converted from the SPAC coefficients the phase velocities show their availability by themselves in the following way. Plotted against the frequency, they start growing with unacceptably low value, take a first peak then gradually decrease, take the minimum value and finally increase to unacceptably high value. The frequency range between these peaks and the minimums is extracted at first.

In the second step, the frequency range that corresponds to the wave length longer than  $2D$  and shorter than  $5D$  is extracted, where  $D$  denotes the inter station interval. The former corresponds to the Nyquist wave length (Okada 2006), whereas the latter is the border between acceptable and critical range (Cornou *et al.* 2006). For a four station array, one at the center and others equally distributed on a circle, the maximum inter station interval  $D_{max}$  is equal to  $1.732D$ . Therefore  $5D$  approximately corresponds to  $3D_{max}$ . This criterion is applied to each inter station interval independently and a set of the extracted dispersion curves are obtained.

#### 4.2.1 N101 case

The theoretical curve calculated using Eqn.(3.5) is shown in Figure 4.2 *left* together with those of the fundamental and the first higher modes (black broken, black solid and gray curves respectively). I propose to call this theoretical phase velocities *false velocities*, because these do not correspond to any elastic waves. Namely, these are ghosts produced by the assumption of single mode to the real data that is of multiple modes. Figure 4.2 *right* shows its very good coincidence with the observed one shown in Figure 4.1 *right*. The fall off at the low frequency can be considered as the consequence of the ability of CCA using this small size array.

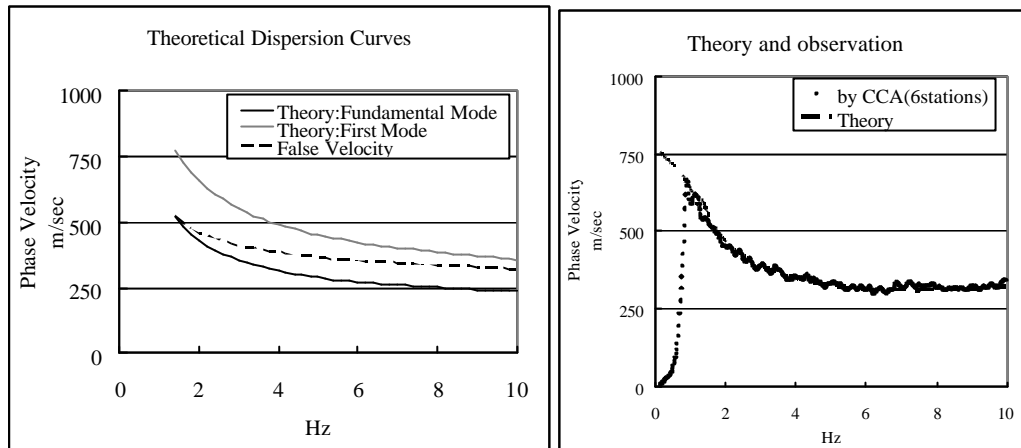


Figure 4.2. N101 Case. *Left*: Theoretical dispersion curve based on Eqn.(3.5) for  $r=6m$  in comparison with the fundamental and the first higher modes (black broken, black solid and gray curves respectively). *Right*: Comparison of theoretical dispersion curve with the observed one (broken curve and dots respectively).

#### 4.2.2 N104 case

The dataset N104 is composed of the records obtained by the triangular arrays of which radii are about 12m, 23m, 47m, 180m, 350m and 700m. The observed dispersion curve is obtained by the conventional way of SPAC. Then, theoretical one is modeled using Eqn.(3.5).

Eqn.(3.5) foresees the theoretical dispersion curve influenced by the fundamental and the first higher modes as shown in Figure 4.3 *left* (broken, black and gray curves respectively). This complicated behavior, however, coincide well to the observed one as shown in Figure 4.3 *right*.

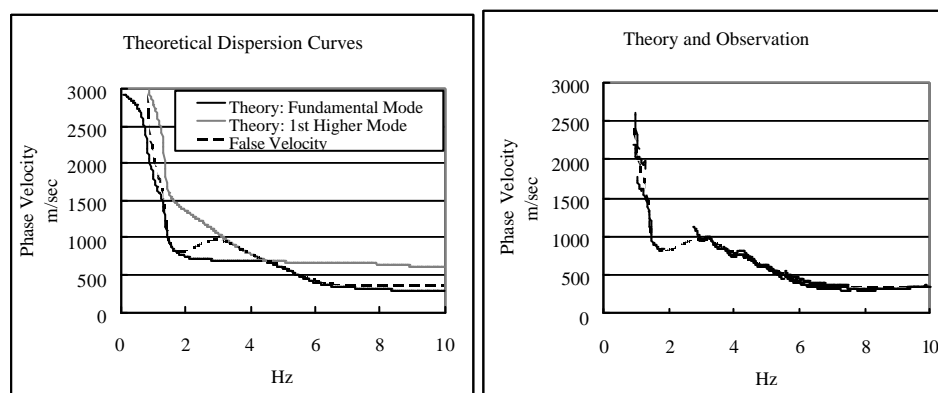


Figure 4.3 N104 case. *Left*: Theoretical dispersion curve based on Eqn.(3.5) in comparison with the fundamental and the first higher modes (black broken, black solid and gray curves respectively). *Right*: Its comparison with the observed one. The smooth broken curve is the theoretical one.

## 5. DISCUSSION

It is obviously observed that in Figure 4.3 *right* there is theoretical curve alone in the frequency range between about 2.0Hz to about 3.0Hz. This is caused by the usage of the above mentioned procedure that extracts the part of the dispersion curve where the phase velocity decreases with the frequency. The mentioned frequency range that has a positive gradient against the frequency is automatically eliminated by this procedure. More specifically, this elimination is controlled by the threshold value at longer wave length side, *i. e.*, the wave length is less than  $3D_{max}$ . This threshold value is not determined strictly but can be changed due to the balance of coherent and incoherent signals. Therefore it is difficult to say that  $3D_{max}$  is the most appropriate for every case. Gouédard *et al.* (2008) describes that many authors has reported for SPAC the maximum resolvable wave length is in the order of  $5D_{max}$  to  $7.5D_{max}$ . The criterion used for Figure 4.3 *right* is relatively conservative.

It is pointed out by Wapenaar and Fokkema (2006) that the retrieval of amplitude requires much longer records than that of the phase. It is clearly shown that the square of the normalized eigen function of the fundamental to that of the first higher modes play an important role to determine the false velocity in the frequency range from 2.0Hz to 4.0Hz. In this transient range the convergence of the observed dispersion curves is looser than the other parts. This observation seems consistent with this theoretical foreseen of Seismic Interferometry. Because the amplitudes are used in Eqn.(3.5), the threshold of the maximum resolvable wave length seems to have to be same or similar as that for other methods using information of amplitude, *e. g.*, the frequency wavenumber method, that is  $3D_{max}$  (*e. g.*, Gouédard *et al.* 2008).

The presence of the first higher mode can be detected easily during analysis in N104 case because it causes a difficulty in fitting the observed SPAC coefficients to  $J_0(kr)$ , whereas in N101 case it is almost impossible to detect it from observed dispersion curve and the fitting to the theoretical dispersion curve of fundamental mode may be performed without any doubt. Therefore N101 seems more dangerous. Note that the analysis of SPAC has been done for long time on the assumption of the presence of the fundamental mode alone. It seems that some of them may contain the error due to the influence of the first higher mode especially in the frequency range higher than few Hz in that the mixture of the first higher mode is inevitable.

## 6. CONCLUSIONS

In this paper, we have shown the theoretically the consistency of SPAC with Seismic Interferometry and have conducted numerical experiments using the simulated microtremor records that include both of the fundamental and the first higher modes of Rayleigh waves in order to confirm the formulas foreseen by the Seismic Interferometry to calculate the phase velocity. First, an example is shown using N101 for that CCA with small array can provide the coincident dispersion curve to that given by SPAC with much larger array. These, however, run off systematically from the theoretical one of the fundamental mode. Then, two examples are shown using N101 and N104 for that the observed dispersion curves affected by the first higher mode can be reproduced based on Eqn.(3.5) that is one of the consequence of the hypothesis of Seismic Interferometry. These results clearly show that the proposed formula, *i. e.*, Eqn.(3.5) is the way to estimate the influence of the first higher mode on the observed dispersion curve. On the other hand, the hypothesis of Seismic Interferometry obtained an example that supports its appropriateness.

## REFERENCES

- Aki, K. (1957). Space and time spectra of stationary stochastic waves, with special reference to microtremors, *Bull. Earthq. Res. Inst. Univ. Tokyo*, **35**, 415–457.
- Aki, K. and Richard, P. G. (2002). *Quantitative Seismology*, 2nd Edition, University Science Books, California
- Asten, M.W. (2006). On bias and noise in passive seismic data from finite circular array data processed using SPAC methods, *Geophysics*, **71**, V153-V162
- Bettig, B., Bard, P.-Y., Scherbaum, F., Riepl, J., Cotton, F., Cornou, C. and Harzfeld, D., (2001). Analysis of dense array noise measurements using the modified spatial auto-correlation method MSPAC- application to the Grenoble area, *Bolletino di Geofisica Teorica e Applicata*, **42**, 281-304.

- Chavez-Garcia, F. J., Rodriguez, M. and Stephenson, W. R. (2005). An Alternative Approach to the SPAC Analysis of Microtremors: Exploiting Stationarity of Noise, *Bull. Seism. Soc. Am.*, **95**, 277-293.
- Chavez-Garcia, F. J., Rodriguez, M. and Stephenson, W. R., (2006). Subsoil Structure Using SPAC Measurements along a Line, *Bull. Seism. Soc. Am.*, **96**, 729-736.
- Cho, I., Tada, T. and Shinozaki, Y., (2006a). Centerless circular array method: Inferring phase velocities of Rayleigh waves in broad wavelength ranges using microtremor records, *Jour. Geophys. Res.*, **111**, B09315.
- Cho, I., Tada, T. and Shinozaki, Y., (2006b). A generic formulation for microtremor exploration methods using three component records from a circular array, *Geophys. J. Int.*, **165**, 236-258.
- Clearbout, J. F., (1968). Synthesis of a layered medium from its acoustic transmission response, *Geophysics*, **33**, 264-269.
- Cornou, C., Ohrnberger, M., Boore, D. M., Kudo, K. and Bard, P.-Y., (2006). Derivation of Structural Models from Ambient Vibration Array Recordings: Result from an Interpretational Blind Test, in *Proc. 3<sup>rd</sup> Int. Symp. on the Effects of Surface Geology on Seismic Motion, Grenoble, France, 29 August – 1 September, 2006*, eds Bard, P.-Y., Chaljub, E., Cornou, C., Cotton, F. and Gueguen, P., LCPC Editions, Paper Number: NBT.
- Gouédard, P., Cornou, C. and Roux, P., (2008). Phase-Velocity Dispersion Curves and Small-Scale Geophysics using Noise Correlation Slantstack Technique, *Geophys. J. Int.*, **172**, 971-981.
- Köhler, A., Ohrnberger, M., Scherbaum, F., Wathlet, M. and Cornou, C. (2007). Assessing the reliability of the modified three-component spatial autocorrelation technique, *Geophys. J. Int.*, **168**, 779-796.
- Moczo, P. and Kristek, J. (2002). "FD code to generate noise synthetics", Sesame report D02.09, available on <http://SESAME-FP5.obs.ujf-grenoble.fr>
- Morikawa, H., Sawada, S. and Akamatsu, J. (2004). A Method to Estimate Phase Velocities of Rayleigh Waves Using Microtremors Simultaneously Observed at Two Sites, *Bull. Seism. Soc. Am.*, **94**, 961-976.
- Ohori, M., Nobata, A. and Wakamatsu, K. (2002). A comparison of ESAC and FK methods of estimating phase velocity using arbitrarily shaped microtremor arrays, *Bull. Seism. Soc. Am.*, **92**, 2323-2332.
- Ohrnberger, M., Schisslie, E., Cornou, C., Bonnefoy-Claudet, S., Wathelet, M., Savvaidis, A., Scherbaum, A. and Jongmans, D. (2004). Frequency Wavenumber and Spatial Autocorrelation Methods for Dispersion Curve Determination from Ambient Vibration Recordings, *Proc. of 13th World Conference on Earthquake Engineering*, Paper No. 0946.
- Okada, H. (2003). The Microtremor Survey Method, Geophysical Monograph, No. 12, Society of Exploration Geophysicists, Tulsa.
- Okada, H., (2006). The efficient number of stations required by circular array for the spatial auto-correlation method applied to array observations of microtremors: Joint publication of *Exploration Geophysics*, **37**, 73-85.
- Sabra, K., Gerstoft, G.P., Roux, P. and Kuperman, W. A. (2005a). Extracting time-domain Green's function estimates from ambient seismic noise, *Geophys. Res. Lett.*, **32**, L03310.
- Sabra, K., Gerstoft, G.P., Roux, P. and Kuperman, W. A. (2005b). Surface wave tomography from microseisms in Southern California, *Geophys. Res. Lett.*, **32**, L14311
- Sanchez-Sesma, F. J. and Campillo, M. (2006). Retrieval of the Green's Function from Cross Correlation: The Canonical Elastic Problem, *Bull. Seism. Soc. Am.*, **96**, 1182-1192.
- Shapiro, N. M., Campillo, M., Stehly, L. and Ritzwoller, M. H., 2005, High-Resolution Surface wave Tomography from Ambient Seismic Noise, *Science*, **307**, 1615-1618.
- Snieder, R. (2004). Extracting the Green's function from the correlation of coda waves: A derivation based on stationary phase, *Phys. Rev. E* **69**, 046610.
- Tada, T., Cho, I. and Shinozaki, Y. (2007). Beyond the SPAC method: Exploiting the Wealth of Circular-Array Methods for Microtremor Exploration, *Bull. Seism. Soc. Am.*, **97**, 2080-2095.
- Tokimatsu, K., Tamura, S. and Kojima, K. (1992). Effects of Multiple Mode on Rayleigh Wave Dispersion Characteristics, *Jour. Geotech. Engn.*, **118**, 1529-1543.
- Wapenaar, K. and Fokkema, J. (2006). Green's Function Representations for Seismic Interferometry, *Geophysics*, **71**, SI33-SI46.
- Wapenaar, K., Draganov, D. and Robertson, J., (2006). Introduction to the supplementary to Seismic Interferometry, *Geophysics*, **71**, SI1-SI4.
- Yokoi, T. and Margaryan, S. (2008). Consistency of Spatial Autocorrelation Method with the Seismic Interferometry and Its Consequence, *Geophys. Prospecting*, **56**, 435-451.